HHS Public Access

Author manuscript

Dent Mater. Author manuscript; available in PMC 2016 November 01.

Published in final edited form as:

Dent Mater. 2015 November ; 31(11): 1304–1311. doi:10.1016/j.dental.2015.08.161.

On the interfacial fracture resistance of resin-bonded zirconia and glass-infiltrated graded zirconia

Herzl Chai[1], **Marina Kaizer**[2,3], **Asima Chughtai**[2], **Hui Tong**[2,4], **Carina Tanaka**[2,5], and **Yu Zhang**[2]

[1]Tel Aviv University, School of Mechanical Engineering, Faculty of Engineering, Tel Aviv, Israel

[2]New York University College of Dentistry, Department of Biomaterials and Biomimetics, 433 First Avenue, Room 810, New York, NY 10010, USA

[3]Federal University of Pelotas, Graduate Program in Dentistry, Pelotas, Brazil

[4]School of Metallurgy and Environment, Central South University, Changsha, Hunan 410083, P.R. China

[5]Department of Biomaterial and Oral Biology, School of Dentistry, University of São Paulo, São Paulo, Brazil

Abstract

Objective—A major limiting factor for the widespread use of zirconia in prosthetic dentistry is its poor resin-cement bonding capabilities. We show that this deficiency can be overcome by infiltrating the zirconia cementation surface with glass. Current methods for assessing the fracture resistance of resin-ceramic bonds are marred by uneven stress distribution at the interface, which may result in erroneous interfacial fracture resistance values. We have applied a wedge-loaded double-cantilever-beam testing approach to accurately measure the interfacial fracture resistance of adhesively bonded zirconia-based restorative materials.

Methods—The interfacial fracture energy G_C was determined for adhesively bonded zirconia, graded zirconia and feldspathic ceramic bars. The bonding surfaces were subjected to sandblasting or acid etching treatments. Baseline G_C was measured for bonded specimens subjected to 7 days hydration at 37 °C. Long-term G_C was determined for specimens exposed to 20,000 thermal cycles between 5 and 55 °C followed by 2-month aging at 37 °C in water. The test data were interpreted with the aid of a 2D finite element fracture analysis.

Results—The baseline and long-term G_C for graded zirconia was 2–3 and 8 times that for zirconia, respectively. More significantly, both the baseline and long-term G_C of graded zirconia were similar to those for feldspathic ceramic.

*corresponding author, 433 First Avenue, Room 810, Department of Biomaterials and Biomimetics, New York University College of Dentistry, New York, NY 10010, Tel.: (212) 998-9637, Fax: (212) 995-4244, yz21@nyu.edu.

Significance—The interfacial fracture energy of feldspathic ceramic and graded zirconia was controlled by the fracture energy of the resin cement while that of zirconia by the interface. G_C for the graded zirconia was as large as for feldspathic ceramic, making it an attractive material for use in dentistry.

Keywords

Cement bond; interfacial fracture energy; zirconia; glass-infiltrated graded zirconia; feldspathic ceramic; wedge-loaded double-cantilever-beam

1. Introduction

In recent years zirconia has emerged as a promising restorative material for dental crowns and fixed dental prostheses due to its superior mechanical properties and excellent biocompatibility. However, owing to its chemical inertness zirconia suffers from poor bonding to adhesive resin cements, which greatly limits its applications in adhesively bonded dental restorative prostheses such as Maryland bridges, cantilever bridges, partial crowns, inlays and onlays. Several surface treatment approaches for improving zirconia-resin bonding were offered which may be categorized as mechanical, chemical or a combination of both. Successful examples for mechanical treatments are sandblasting with alumina particles [1–3] and porous nano-structured alumina coating [4–6], whereas those for chemical treatments include thin silica-based coatings [7,8] and surface functionalization using various chemical treatments [9,10]. Chemo-mechanical treatments have also been widely used for this purpose, including co-jet sandblasting [11] and more recently surface glass-infiltration [12,13]. It has been reported that modification of zirconia surface by glass-infiltration improves the esthetics of dental crowns [14], as well as flexural strength [6,15–17] and resistance to veneer/core delamination [18] yet without compromising key mechanical properties such as resistance to occlusal cracking [14,19] and edge chipping [20,21]. An important benefit of this approach in the present context is that it provides a glass rich surface that allows the application of standard etching-silane cementation techniques. The resin-cement bonding quality of the surface of the glass-infiltrated graded zirconia, the latter to be referred here as “graded zirconia", has not been examined, however.

A number of testing approaches for evaluating bond strength in applications to restorative prosthetic materials have been suggested, the most commonly used in adhesive dentistry being the Shear Bond Strength (SBS) and Microtensile Bond Strength (MTBS) (e.g., [22–24]). Such methods have been used to evaluate the effect of surface treatment or thermocycling of ceramic restorative materials [25,26]; thermocycling has been used extensively to simulate aging of resin cement in an intra-oral environment [9,27]. While relatively simple, such testing concepts are generally marred by large variations in the bond failure stress, the effect that may be attributed to the joint's sensitivity to geometric misalignments and the tendency for tensile stresses to concentrate at the bond terminus [28,29]. An alternative means for assessing bond strength is the use of fracture mechanics. In this approach the bond includes an initial crack starter which facilitates a smooth crack initiation and growth thus eliminating the sensitivity to flaws and stress gradients and reducing the effect of geometric misalignments. The quantity of interest in this case is the

fracture energy (per unit area) needed to extend the starting crack, G_C, rather than the failure stress. A popular means for evaluating G_C in applications to adhesively bonded joints is the double-cantilever-beam (DCB) specimen. In this case the bond is subjected to tensile stress at the crack tip, which is generally associated with the most critical form of fracture [30]. In addition to the relative ease in specimen fabrication and testing, the calculated fracture energy is little sensitive to the cement layer thickness [30,31], which may vary greatly in a clinical setting.

In this work we examined the efficacy of surface glass-infiltration on the resin-cement bond properties of zirconia. The interfacial fracture energy was determined using the DCB specimen. Both short-term (7 days hydration at 37 °C) and long-term (20,000 thermal cycles between 5 °C and 55 °C followed by a 2-month aging at 37 °C) in vitro simulations were considered. A widely used commercial dental feldspathic ceramic was chosen as a reference bonding material.

2. Materials and Methods

Figure 1 shows the wedge double-cantilever-beam specimen (WDCB) used. Details of the fabrication and testing procedures follow.

2.1 Materials

Three ceramic restorative materials were tested: zirconia, graded zirconia and feldspathic ceramic. The zirconia (5.18 wt.% Y_2O_3, TZ-3Y-E grade, Tosoh, Tokyo, Japan) specimens were fabricated from cold isostatic pressed and lightly sintered tiles (14 × 35 × 80 mm). The tiles were cut into 3.8 × 3.8 × 35 mm bars and sintered at 1450 °C for 2 h. The preparation of graded zirconia has been described earlier [13]. Briefly, an in-house developed glass with composition similar to dental porcelain and CTE machting that of the zirconia (10. 5×10^{-6} °C) was prepared. The main composition of the glass by weight was 65.5% SiO_2, 11.7% Al_2O_3, 10.0% K_2O, 7.3% Na_2O, 3.0% CaO. The glass, in the form of powder slurry, was first applied on pre-sintered Y-TZP bars (1350 °C for 1 h). Glass-infiltration and densification occurred in a single process at 1450 °C for 2 h. The resulting structure consisted of a 15 to 40 μm thick residual glass layer followed by a 120 μm thick graded layer where the content of intergranular glass gradually diminishes and finally transitioned into a dense Y-TZP interior. All specimen surfaces except for the cementation ones were grind and polished down to 6 μm grade finish, resulting in the following final dimensions for the zirconia and graded zirconia: (b, h, L) = (3, 3, 30) mm where, as shown in Fig. 1, b, h and L are the depth, thickness and length of the specimen bars, in that order. The feldspathic ceramic bars were cut from commercial large CAD/CAM blocks (VITABLOCS TriLuxe forte, a fine-structure feldspar ceramic). As for zirconia, all surfaces except for the cementation ones were polished down to 6 μm grade finish. The specimen final dimensions for feldspathic ceramic were (b, h, L) = (3, 5, 30) mm. To guide the insertion of a crack opening wedge, prior to bonding the top edges of the cementation surfaces of all bar specimens were beveled at 45° relative to the long axis of the beam (Fig. 1) by means of grinding using 10 μm diamond impregnated polishing discs under water cooling. The vertical length of the beveled region was set at 1 mm. Since the bond-normal (F_x) and

compressive (F_y) load components transmitted to the specimen edge are unaffected by this edge beveling, and the crack tip is at least 4 mm away from the beveled edges, the effect of material beveling on the measured G_C value is deemed negligible. The cementation surface of zirconia and graded zirconia were kept in their sintered and infiltrated stage, respectively, whereas those of feldspathic ceramic were abraded with 15 μm diamond disc in preparation for further surface treatments, i.e. acid etching or sandblasting.

2.2 Cementation

One-hundred cemented specimens (5 Groups, $n = 20$) were prepared by adhesive cementation of two identical ceramic bars with a ten-methacryloyloxydecyl dihydrogen phosphate (MDP) containing dental cement (Panavia F 2.0, Kuraray, Osaka, Japan). The selection of this cement was motivated by a previous study showing that the MDP-containing composite resin cement Panavia F coupled with a sandblasted zirconia surface gives rise to a long-term durable bond [32]. The cementation surfaces of the ceramic bars were subject to sandblasting or acid etching, commonly used practices for enhancing bond strength [32–36]. The specimens in each of the five groups were categorized based on surface preparation and ceramic materials as follows: Groups 1, 2 and 3 - zirconia (Yttria-tetragonal zirconia polycrystals), graded zirconia, and feldspathic ceramic (VITABLOCS TriLuxe forte), in that order, each sandblasted with aluminum oxide (Al_2O_3) particles; Group 4 - graded zirconia acid etched with 5% hydrofluoric acid (VITA Ceramic Etch) for 2 min; Group 5 - feldspathic ceramic acid etched with 5% hydrofluoric acid (VITA Ceramic Etch) for 1 min. The parameters for sandblasting were: 50 μm alumina particles at 1 bar for graded zirconia and feldspathic ceramic, and 2 bars for zirconia, 1 cm stand-off distance and 2 s per cm^2.

After surface treatment, the cementation protocol followed manufacturer's instructions for Panavia F 2.0. All bars were cleaned using distilled water in an ultrasonic bath (Solid state/ ultrasonic T-14B, L&R, New Jersey, USA) for 2 minutes. A thin layer of K-etchant gel (Kuraray, Osaka, Japan) was applied to the cementation surface with a small micro-brush. After 5 s, the layer was washed thoroughly and the bars dried with oil- and moisture-free compressed air. Clearfil Ceramic Primer (Kuraray, Osaka, Japan), an MDP containing coupling agent, was applied to the prepared surface of the bar with a micro-brush and dispersed with oil- and moisture-free air stream for 5 s.

A 50 μm thick aluminum foil was placed at the end of the beveled edge of one of the two bonding bars to help control the thickness of cement between the bars. Equal amounts of paste A and Paste B of Panavia F 2.0 were mixed with a spatula for 20 s after which the mixture was applied to the bonding surface. The two bars were then pressed together for 30 s using a force of 9.8 N. After removing the aluminum foil, the bonding surfaces were light cured for 20 s (Ultra Lume LED 5, UT, US). The cemented bars were stored in distilled water at 37 °C in an incubator for a period of 7 days in order to hydrate the cement [37,38].

After curing the surface of the observed edge of the bond was polished with a 6 μm diamond suspension. The adhesive thickness, measured along the bonded interface using an optical microscope, typically varied from 50 to 80 μm. A cut ~0.5 mm deep was created along the bond line, just below the beveled edges, using a 0.3 mm thick diamond impregnated wheel

soaked in water coolant. The introduction of this narrow cut was to help start a smooth crack growth.

2.3 Thermocycling and storage

The specimens in each group (5 groups, $n = 20$) were subjected to 2 different storage conditions before testing: (1) 7 days incubation in distilled water at 37 °C (5 groups, $n = 10$); (2) 20,000 thermal cycles between 5 °C to 55 °C and 60 days incubation at 37 °C (5 groups, $n = 10$). The thermal cycle treatments were carried out by alternately submerging the bonded specimens between two water baths of 5 °C and 55 °C with a dwell time of 30 s at each temperature. Note that 20,000 cycles have been estimated to be equivalent to a period of 2 years in the oral cavity [39]. To further simulate intraoral conditions, all thermocycled specimens were stored in the incubator for an additional 60 days at 37°C [40].

2.4 Testing

Figure 1 shows the specimen in the loading stage. The lower part of the specimens was firmly gripped by a vice over a distance $e = 8$ mm while the upper part pressed down by a hardened steel wedge of total angle $2\beta = 60°$ at a constant displacement rate of 0.1 mm/min using a standard loading frame. The evolution of cracking was observed from the polished specimen edge using a video camera equipped with a telescopic lens (Optem, Inc.). To help locate the crack tip, a paper scale bar was glued along the bonded interface prior to loading. After unloading, the fracture surfaces were observed with an optical microscope or a scanning electron microscope (SEM). From the video footage and machine output the load P_i to initiate rapid fracture and corresponding crack length c_i were documented for each test.

2.5 Fracture energy calculation

The variation of energy release rate G (energy per unit area) with crack length c for the specimen shown in Fig. 1 was determined using a commercial FEM code (Ansys Inc.) specified to plane strain conditions. Because of its relative smallness, the adhesive thickness was neglected in the calculations. From dimensional consideration the energy release rate G takes the form (e.g., [41])

$$GEhb^2/P^2 = f(c/h) \quad (1)$$

where P is the applied load, E is the Young's modulus of the bar and f is some function of c/h. Assuming, for simplicity, that the load from the wedge is transmitted to the specimen arms by frictionless contact, it can be easily shown that the horizontal and vertical components of the applied load per unit specimen width, F_x and F_y, respectively, are given by:

$$F_y = P/2b, F_x = (P/2b)\tan\beta \quad (2)$$

The energy release rate in the specimen was determined using Irwin's crack opening displacement approach:

$$G = [\pi/8(1-\nu^2)]u^2E/\Delta \quad (3)$$

where ν is the adherend's Poisson's ratio, Δ the size of the square FEM grid at the crack tip and *u* the total crack opening displacement associated with the grid at the crack tip. Table 1 lists the elastic constants used in this study. The quantity in the right hand side of Eq. 3 was calculated for the pertaining case β = 30° with *b*, *h*, *E* and *P* each taken as unity (for which $G = f$). The FEM mesh was refined until *G* converged to within 2–3%.

2.6 Statistical analysis

The fracture energy (G_C) data were analyzed by two-way ANOVA (General Linear Model – GLM) based on Time (Baseline and Aged) and Groups (Z-SB, GZ-SB, GZ-E, P-SB, and P-E). All pairwise multiple comparisons were performed by using Tukey test. The significance level was set at p = 0.05 for all analyses.

3. Results

3.1 FEA

Fig. 2 plots normalized energy release rate $f(c/h)$ vs. normalized crack length c/h for ν = 0.3, where symbols denote FEA data and solid line is a corresponding smooth fit. As shown *f* exhibits a reversal in trends as c/h is increased, from that of a wedge type specimen for which *f* reduces with c/h (i.e., as $G \sim 1/c$, [41]), to a beam-like specimen, where $G \sim c^2$ [31].

3.2 Fracture energy

Fig. 3 shows two selected frames from a video footage for feldspathic ceramic/cement/feldspathic ceramic which typifies the general behavior observed. The bright line at the specimen center indicates a crack. As the wedge load increases from zero, the crack faces open up, making the initial crack visible. (a) With increasing load the crack grows slowly a small distance before a rapid fracture occurs; frame (b) is just before this event.

By using in Fig. 2 pairs of fracture load P_i and corresponding crack length at onset of fast cracking c_i, and beam width *b* and the elastic constants in Table 1, the fracture energy G_C could be found. The crack length c_i was determined from postmortem inspection of the fractured surface with the aid of a stereo microscope. The results show that this quantity was essentially coincident with the edge of the crack starter as well as with the video records. Fig. 4 summarizes the mean and standard deviation values obtained for each of the five groups of specimens tested, where the unshaded and shaded bars correspond to the baseline specimens and those subjected to thermocycling/aging treatment, respectively.

Table 2 (or Figure 4) presents the mean and standard deviation values obtained for each of the five groups of specimens tested before and after aging. Two-way ANOVA showed that both factors (Time - p = 0.044; Groups - p = 0.000), as well as the interaction between them (p = 0.000) were significant.

Although showing considerable scatter, the results reveal several major trends:

a. G_C for graded zirconia well exceeds that for zirconia, being quite similar to that of feldspathic ceramic after long-term thermocycling and wet storage.

b. Except for zirconia, the thermocycling and wet storage treatments do not seem to significantly affect G_C.

c. Sandblasting and acid etching treatments yield quite similar G_C values.

To gain insight into the difference in G_C values seen in Fig. 4, the fracture surface of several specimens were examined under the SEM. Fig. 5 exemplifies the results for zirconia, graded zirconia and feldspathic ceramic, all pertaining to sandblasted, thermally cycled/aged specimens. Shown in each case are two micrographs, where the lower image is a magnified view of the circled area of the upper image. The micrographs conclusively correspond to a region slightly ahead of the edge of the crack starter, where a slow crack growth followed by a rapid one occurred. The fracture tended to take place near one of the two interfaces of the joint. The images for the feldspathic ceramic (a) and graded zirconia (b) reveal a non-planar fracture surface where extensive plastic deformation within the bonding interlayer occurred. Such a morphology, referred to in adhesive bonding technology as cohesive type failure, implies that the interface is at least as strong as the neat resin [30,31,42]. In contrast, the fracture surface for zirconia (c) is fairly smooth and tends to occur near one of the two bond interfaces. Such a morphology, termed adhesive type failure, indicates that the interface is weaker than the neat adhesive. The extensive plastic deformation within the adhesive layer seen in in Figs. 5a and 5b is consistent with the associated relatively large fracture energy seen in Table 2 and Fig. 4.

4. Discussion

Infiltration of zirconia cementation surface with glass to create glass rich surface was shown to substantially increase the resin bond strength relative to untreated zirconia, to a level similar to that of feldspathic ceramic. This held true regardless of surface preparation by sandblasting or acid etching, thermocycling and wet storage. Accordingly, this approach emerges as a viable means for overcoming the poor resin-cement bonding properties of zirconia, a major limiting factor for the widespread use of this material in prosthetic dentistry. The glass infiltrated graded zirconia with improved cement bond strength can now extend the clinical indications of zirconia to more conservative treatments, where adhesively bonded partial coverage restorations (e.g., Maryland bridges, cantilever bridges, partial crowns, inlays and onlays) are preferred choices over the traditional full-coverage crowns and fixed dental prostheses in the interest of preserving the tooth structure.

The interfacial fracture resistance of adhesively bonded joints is dictated by such factors as adherend material, preparation of the cemented surfaces, and state of stresses at the crack tip [30,31,43–45]. It was shown in a study of mode I fracture energy G_C of aluminum alloys bonded with an epoxy resin that with a proper surface treatment G_C may exceed that of the neat resin and furthermore be little sensitive to bond thickness t [30,31]. These works also showed that for $t < 50$ μm, which is within the range of luting cement thickness used in restorative prostheses, $G_C \approx 70$ N/m, a value quite similar to those found in the present study for feldspathic ceramic and surface graded zirconia (Fig. 4). Such correspondence may be expected given the cohesive nature of bond failure seen in Figs. 5a and 5b. In the case of zirconia, Fig. 5c shows a rather flat fracture surface indicative of an adhesive type failure, which is in line with the low G_C value seen in Fig. 4. Noting the similarity in G_C values

between sandblasted and acid etched feldspathic ceramic and graded zirconia (Fig. 4), one concludes that it is the presence of the glass phase rather than surface treatment that is responsible for the enhanced bond strength in the graded zirconia.

It is interesting to comment on the effect of thermocycling and wet storage (TCWS) on G_C seen in Table 2 and Fig. 4. The small G_C value for zirconia is attributable to the weakness of the interface, which would permit incursion of water there; humid environment is known to drastically reduce interfacial strength of bonded joints. This is clearly not an issue in the case of feldspathic ceramic where the failure tended to occurs away from the interface, i.e., within the bulk adhesive (Fig. 5a). The behavior for the graded zirconia is more involved. As shown, the G_C values for the TCWS specimens are quite similar to those for feldspathic ceramic, attributable to the presence of the silica glass phase. The difference in G_C between the uncycled and cycled specimens in this case and the reduction in G_C for the etched feldspathic ceramic surfaces due to TCWS in Fig. 4 are not well understood. It is possible that these effects may reflect experimental scatter, which may be caused by aspects that were not accounted here in the interest of simplicity: (a) Often the initial crack exhibits a small growth prior to onset of rapid fracture. In view of Fig. 2, this growth may lead to error for small samples as used here which is not easy to quantify. This undesirable effect can be reduced by increasing the initial crack length (and hence the specimen size) as well as by producing an initial sharp crack, e.g., using cyclic loading. (b) Friction between the loading tool and the sample (c) The adhesive thickness in this work typically ranged from 30 to 80 μm. As shown in [30,31], this would have some effect both on the fracture energy of the bond as well as on the calculations of G_C.

The bond strength in this study was evaluated under tensile type loading (Fig. 1). Bonded restorative prostheses may be subjected to a combination of tension and shear loading, which may significantly affect the fracture energy. Studies show that over the acceptable adhesive cement thickness range used in dental restorations (e.g. 20 to 100 μm) the fracture energy under shear loading (mode II) generally well exceeds that under tensile loading (mode I) [30]. In fact, measuring G_C in shear may require such large a load as to cause failure of ceramic adherends (including zirconia) prior to any crack growth. These reasoning support our mode I specimen choice, which is a combination of the common DCB specimen [42,46,47] and a wedge type compressive loading [41]. The proposed WDCB specimen is especially useful for small ceramic parts which are difficult to machine or to load. It should be noted that for diffusion bonded ceramics, e.g., porcelain fused to zirconia, G_C is generally evaluated under shear dominated loading using the straightforward four-point-bent specimen [18,48,49]. This approach is feasible and meaningful in this case due to the relatively small interfacial fracture energy in diffusion bonded systems.

Figure 4 indicates that following thermocycling treatment G_C tends to reduce for zirconia while increase somewhat for graded zirconia and feldspathic ceramic. The cause for this is not well understood. Thermocycling between 5 °C and 55 °C water baths introduces thermal stresses into the system owing to the difference in coefficient of thermal expansion between ceramic and cement. It is possible that the reduction in zirconia is due to the weakening of the interface by cyclic thermal stressing of the already weak interface. The thermal stressing is less effective in well-bonded graded zirconia and feldspathic ceramic. In fact, a slight

increase in G_C was observed for these materials following thermocycling treatment. A study of resin-bonded and silane treated silica-based ceramics [50] showed a significant increase in the mean tensile bond strength for etched and etched and sandblasted groups after thermocycling. Such an improvement may be attributed to post-curing of the resin due to the elevated temperature used [50].

5. Conclusions

Infiltration of glass into the zirconia surface was found to increase the mode I fracture energy G_C of the joint by a factor of ~3, to a level consistent with feldspathic ceramic. This finding, together with the increased resistance to occlusal cracking, edge chipping and delamination found earlier, tend to confirm that graded zirconia is a promising dental restorative material. The WDCB specimen developed and implemented in this work provides a viable means for assessing bond strength of ceramic dental materials. This testing approach yields quite reproducible G_C values for the most critical mode I loading yet without the need to measure crack length.

Acknowledgements

This work was sponsored by funding from the United States National Institute of Dental & Craniofacial Research, National Institutes of Health (P.I. Y. Zhang, Grant 2R01 DE017925) and the Israeli Science Foundation (P.I. H. Chai, ISF Grant no. 810/09).

References

1. Kosmac T, Oblak C, Jevnikar P, Funduk N, Marion L. The effect of surface grinding and sandblasting on flexural strength and reliability of y-tzp zirconia ceramic. Dent Mater. 1999; 15:426–433. [PubMed: 10863444]
2. Zhang Y, Lawn BR, Malament KA, Van Thompson P, Rekow ED. Damage accumulation and fatigue life of particle-abraded ceramics. Int J Prosthodont. 2006; 19:442–448. [PubMed: 17323721]
3. Zhang Y, Lawn BR, Rekow ED, Thompson VP. Effect of sandblasting on the long-term performance of dental ceramics. J Biomed Mater Res B Appl Biomater. 2004; 71:381–386. [PubMed: 15386395]
4. Jevnikar P, Krnel K, Kocjan A, Funduk N, Kosmac T. The effect of nano-structured alumina coating on resin-bond strength to zirconia ceramics. Dent Mater. 2010; 26:688–696. [PubMed: 20381854]
5. Kocjan A, Dakskobler A, Kosmac T. Superhydrophobic nanostructured boehmite coatings prepared by aln powder hydrolysis. Int J Appl Ceram Tec. 2011; 8:848–853.
6. Srikanth R, Kosmac T, Della Bona A, Yin L, Zhang Y. Effects of cementation surface modifications on fracture resistance of zirconia. Dent Mater. 2015; 31:435–442. [PubMed: 25687628]
7. Piascik JR, Swift EJ, Thompson JY, Grego S, Stoner BR. Surface modification for enhanced silanation of zirconia ceramics. Dent Mater. 2009; 25:1116–1121. [PubMed: 19376572]
8. Queiroz JR, Massi M, Nogueira L Jr, Sobrinho AS, Bottino MA, Ozcan M. Silica-based nano-coating on zirconia surfaces using reactive magnetron sputtering: Effect on chemical adhesion of resin cements. J Adhes Dent. 2013; 15:151–159. [PubMed: 23534024]
9. Kern M, Wegner SM. Bonding to zirconia ceramic: Adhesion methods and their durability. Dent Mater. 1998; 14:64–71. [PubMed: 9972153]
10. Oliveira-Ogliari A, Collares FM, Feitosa VP, Sauro S, Ogliari FA, Moraes RR. Methacrylate bonding to zirconia by in situ silica nanoparticle surface deposition. Dent Mater. 2015; 31:68–76. [PubMed: 25498521]

11. Blatz MB, Chiche G, Holst S, Sadan A. Influence of surface treatment and simulated aging on bond strengths of luting agents to zirconia. Quintessence Int. 2007; 38:745–753. [PubMed: 17873981]
12. Zhang Y, Chai H, Lawn BR. Graded structures for all-ceramic restorations. J Dent Res. 2010; 89:417–421. [PubMed: 20200413]
13. Zhang Y, Kim JW. Graded structures for damage resistant and aesthetic all-ceramic restorations. Dent Mater. 2009; 25:781–790. [PubMed: 19187955]
14. Ren L, Janal MN, Zhang Y. Sliding contact fatigue of graded zirconia with external esthetic glass. J Dent Res. 2011; 90:1116–1121. [PubMed: 21666105]
15. Zhang Y. Overview: Damage resistance of graded ceramic restorative materials. J Eur Ceram Soc. 2012; 32:2623–2632. [PubMed: 22778494]
16. Zhang Y, Ma L. Optimization of ceramic strength using elastic gradients. Acta Mater. 2009; 57:2721–2729. [PubMed: 20161019]
17. Zhang Y, Sun MJ, Zhang DZ. Designing functionally graded materials with superior load-bearing properties. Acta Biomater. 2012; 8:1101–1108. [PubMed: 22178651]
18. Chai H, Lee JJ, Mieleszko AJ, Chu SJ, Zhang Y. On the interfacial fracture of porcelain/zirconia and graded zirconia dental structures. Acta Biomater. 2014; 10:3756–3761. [PubMed: 24769152]
19. Zhang Y, Kim JW. Graded zirconia glass for resistance to veneer fracture. J Dent Res. 2010; 89:1057–1062. [PubMed: 20651092]
20. Zhang Y, Chai H, Lee JJ, Lawn BR. Chipping resistance of graded zirconia ceramics for dental crowns. J Dent Res. 2012; 91:311–315. [PubMed: 22232142]
21. Zhang Y, Lee JJ, Srikanth R, Lawn BR. Edge chipping and flexural resistance of monolithic ceramics. Dent Mater. 2013; 29:1201–1208. [PubMed: 24139756]
22. Guess PC, Kulis A, Witkowski S, Wolkewitz M, Zhang Y, Strub JR. Shear bond strengths between different zirconia cores and veneering ceramics and their susceptibility to thermocycling. Dent Mater. 2008; 24:1556–1567. [PubMed: 18466964]
23. Sano H, Shono T, Sonoda H, Takatsu T, Ciucchi B, Carvalho R, Pashley DH. Relationship between surface area for adhesion and tensile bond strength — evaluation of a micro-tensile bond test. Dent Mater. 1994; 10:236–240. [PubMed: 7664990]
24. Uhrenbacher J, Schmidlin PR, Keul C, Eichberger M, Roos M, Gernet W, Stawarczyk B. The effect of surface modification on the retention strength of polyetheretherketone crowns adhesively bonded to dentin abutments. J Prosthet Dent. 2014; 112:1489–1497. [PubMed: 24993380]
25. Aboushelib MN, de Kler M, van der Zel JM, Feilzer AJ. Microtensile bond strength and impact energy of fracture of cad-veneered zirconia restorations. J Prosthodont. 2009; 18:211–216. [PubMed: 19141043]
26. Dundar M, Ozcan M, Gokce B, Comlekoglu E, Leite F, Valandro LF. Comparison of two bond strength testing methodologies for bilayered all-ceramics. Dent Mater. 2007; 23:630–636. [PubMed: 16844212]
27. Youngson CC, Jones JC, Fox K, Smith IS, Wood DJ, Gale M. A fluid filtration and clearing technique to assess microleakage associated with three dentine bonding systems. J Dent. 1999; 27:223–233. [PubMed: 10079629]
28. Della Bona A, van Noort R. Shear vs. Tensile bond strength of resin composite bonded to ceramic. J Dent Res. 1995; 74:1591–1596. [PubMed: 7560421]
29. Van Noort R, Noroozi S, Howard IC, Cardew G. A critique of bond strength measurements. J Dent. 1989; 17:61–67. [PubMed: 2659632]
30. Chai H. Shear fracture. Int J Fracture. 1988; 37:137–159.
31. Chai H. On the correlation between the mode i failure of adhesive joints and laminated composites. Eng Fract Mech. 1986; 24:413–431.
32. Wolfart M, Lehmann F, Wolfart S, Kern M. Durability of the resin bond strength to zirconia ceramic after using different surface conditioning methods. Dent Mater. 2007; 23:45–50. [PubMed: 16427692]
33. Kern M, Barloi A, Yang B. Surface conditioning influences zirconia ceramic bonding. J Dent Res. 2009; 88:817–822. [PubMed: 19767578]

34. Ozcan M, Kerkdijk S, Valandro LF. Comparison of resin cement adhesion to y-tzp ceramic following manufacturers' instructions of the cements only. Clin Oral Investig. 2008; 12:279–282.
35. Thurmond JW, Barkmeier WW, Wilwerding TM. Effect of porcelain surface treatments on bond strengths of composite resin bonded to porcelain. J Prosthet Dent. 1994; 72:355–359. [PubMed: 7990039]
36. Della Bona A. Bonding to ceramics: Scientific evidences for clinical dentistry. São Paulo: Artes Médicas. 2009
37. Huang M, Thompson VP, Rekow ED, Soboyejo WO. Modeling of water absorption induced cracks in resin-based composite supported ceramic layer structures. J Biomed Mater Res B Appl Biomater. 2008; 84:124–130. [PubMed: 17497681]
38. Silva NR, de Souza GM, Coelho PG, Stappert CF, Clark EA, Rekow ED, Thompson VP. Effect of water storage time and composite cement thickness on fatigue of a glassceramic trilayer system. J Biomed Mater Res B Appl Biomater. 2008; 84:117–123. [PubMed: 17455281]
39. Gale MS, Darvell BW. Thermal cycling procedures for laboratory testing of dental restorations. J Dent. 1999; 27:89–99. [PubMed: 10071465]
40. Spierings TA, Peters MC, Bosman F, Plasschaert AJ. Verification of theoretical modeling of heat transmission in teeth by in vivo experiments. J Dent Res. 1987; 66:1336–1339. [PubMed: 3476602]
41. Chai H, Ravichandran G. Transverse fracture in multilayers from tension and line-wedge indentation. Int J Fracture. 2007; 145:299–312.
42. Chai H. Bond thickness effect in adhesive joints and its significance for mode i interlaminar fracture of composites. ASTM STP. 1986; 893:209–231.
43. Cao HC, Evans AG. An experimental study of the fracture resistance of bimaterial interfaces. Mech Mater. 1989; 7:295–304.
44. Swadener JG, Liechti KM. Asymmetric shielding mechanisms in the mixed-mode fracture of a glass/epoxy interface. J Appl Mech-T ASME. 1998; 65:25–29.
45. Wang JS, Suo Z. Experimental-determination of interfacial toughness curves using brazil-nut-sandwiches. Acta Metall Mater. 1990; 38:1279–1290.
46. Bascom WD, Cottington RL, Jones RL, Peyser P. The fracture of epoxy- and elastomer-modified epoxy polymers in bulk and as adhesives. J Appl Polym Sci. 1975; 19:2545–2562.
47. Kin Loch AJ, Shaw SJ. The fracture resistance of a toughened epoxy adhesive. J Adhesion. 1981; 12:59–77.
48. Göstemeyer G, Jendras M, Dittmer MP, Bach FW, Stiesch M, Kohorst P. Influence of cooling rate on zirconia/veneer interfacial adhesion. Acta Biomater. 2010; 6:4532–4538. [PubMed: 20601242]
49. Le Thanh R. The University of Sydney. 2009
50. Hooshmand T, van Noort R, Keshvad A. Bond durability of the resin-bonded and silane treated ceramic surface. Dent Mater. 2002; 18:179–188. [PubMed: 11755598]

Highlights

- Infiltrating the zirconia cementation surface with glass can substantially improve its resin bonding strength
- The interfacial fracture energy for glass-infiltrated graded zirconia is similar to that of porcelain
- Current methods for determining the interfacial fracture energy G_C of resin-ceramic bonds are marred by uneven stress distribution at the interface
- A wedge-loaded double-cantilever-beam specimen is developed to accurately measure G_C in adhesively bonded zirconia-based restorative materials

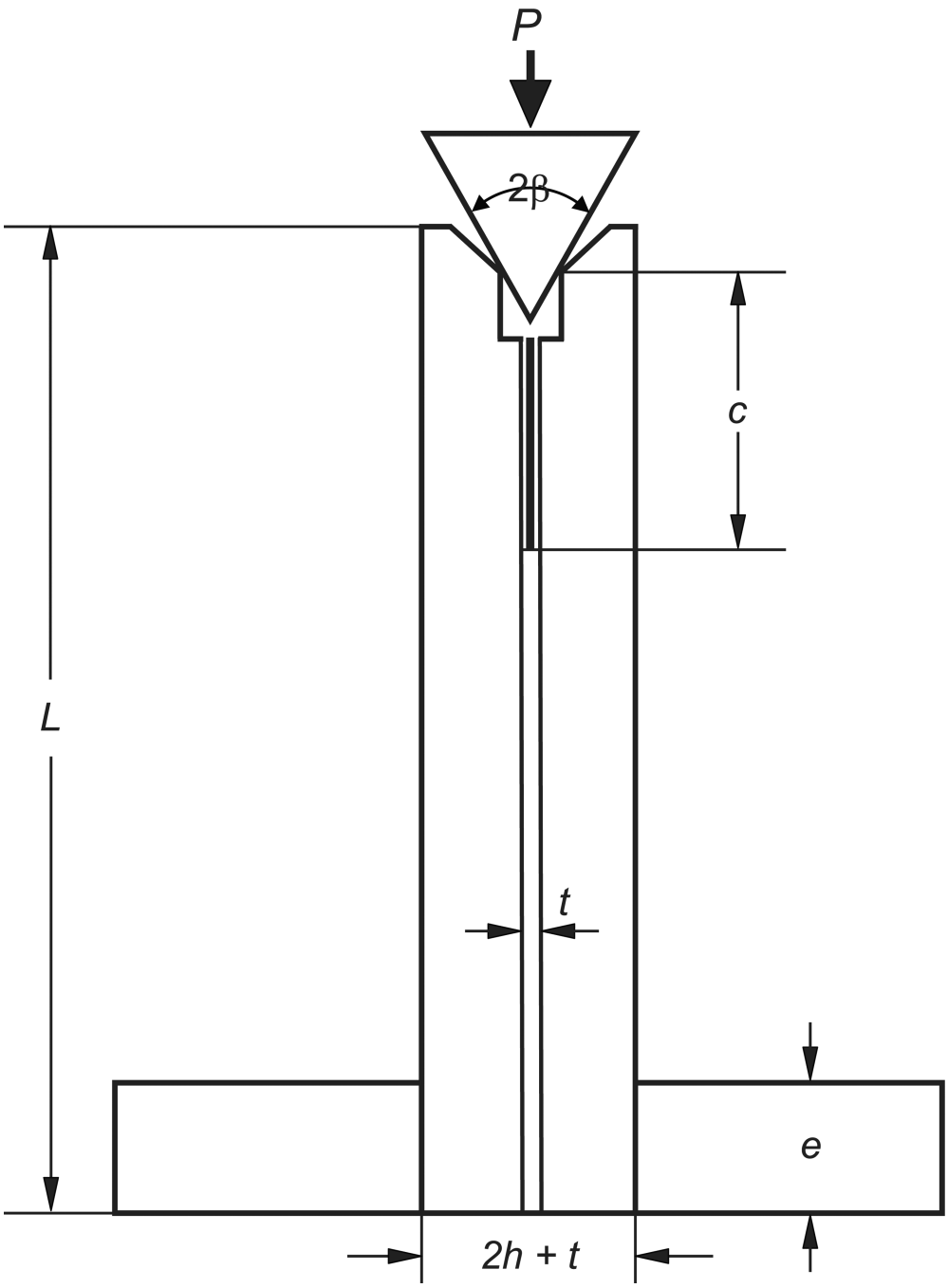

Figure 1.

The wedge double-cantilever-beam (WDCB) adhesive bond specimen used. Pairs of bars (zirconia, graded zirconia, or feldspathic ceramic) are bonded by a resin composite. A crack starter is created using aluminum foil separator. The compression load *P* is applied by a 60° hardened steel wedge which is positioned on a 90° beveled clearance at the specimen edge. This load has a transverse component which opens up the crack faces.

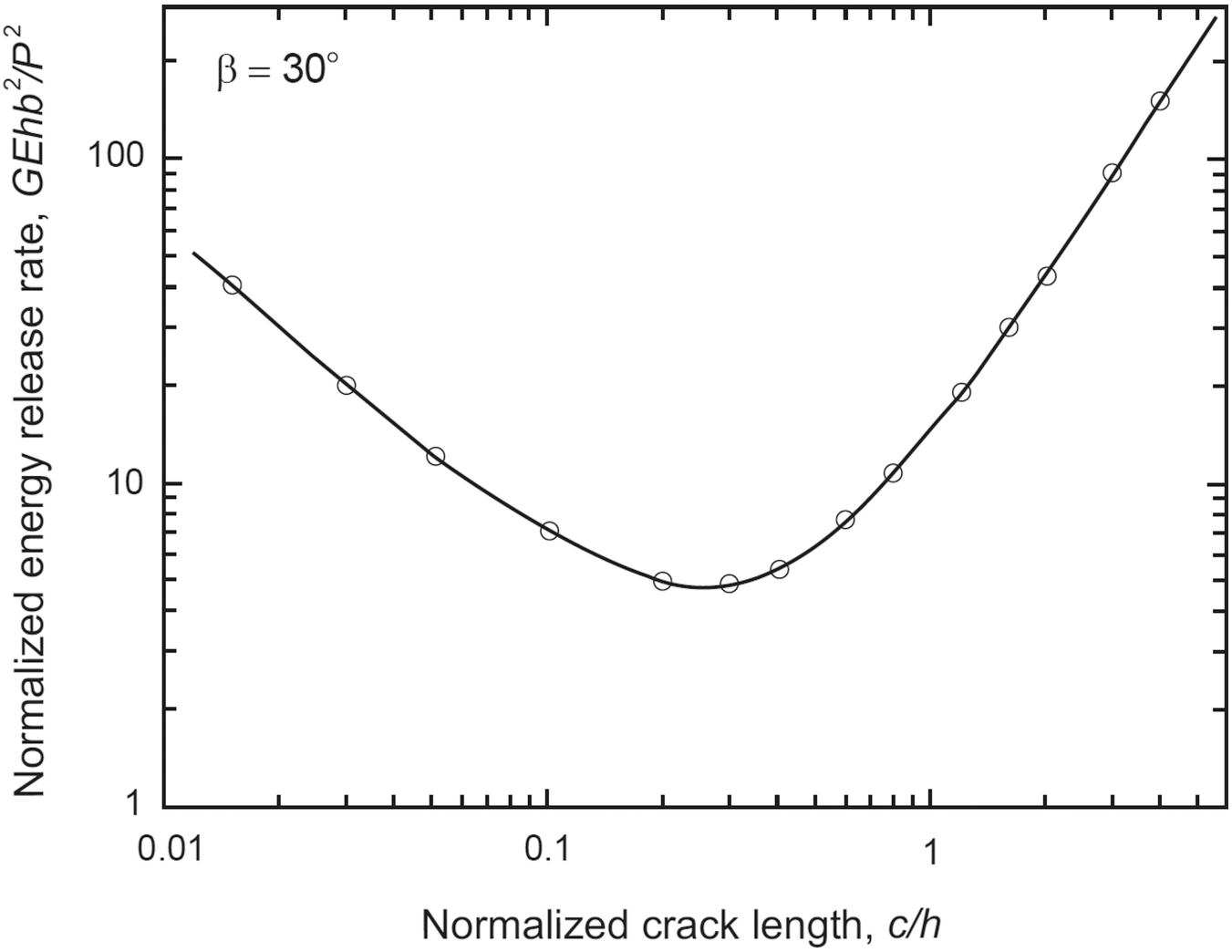

Figure 2.
Normalized energy release rate *G* vs. normalized crack length *c* for the WDCB specimen of Fig. 1, ν = 0.3. Symbols are from the FEM analysis, solid line is a smooth fit to the FEM data.

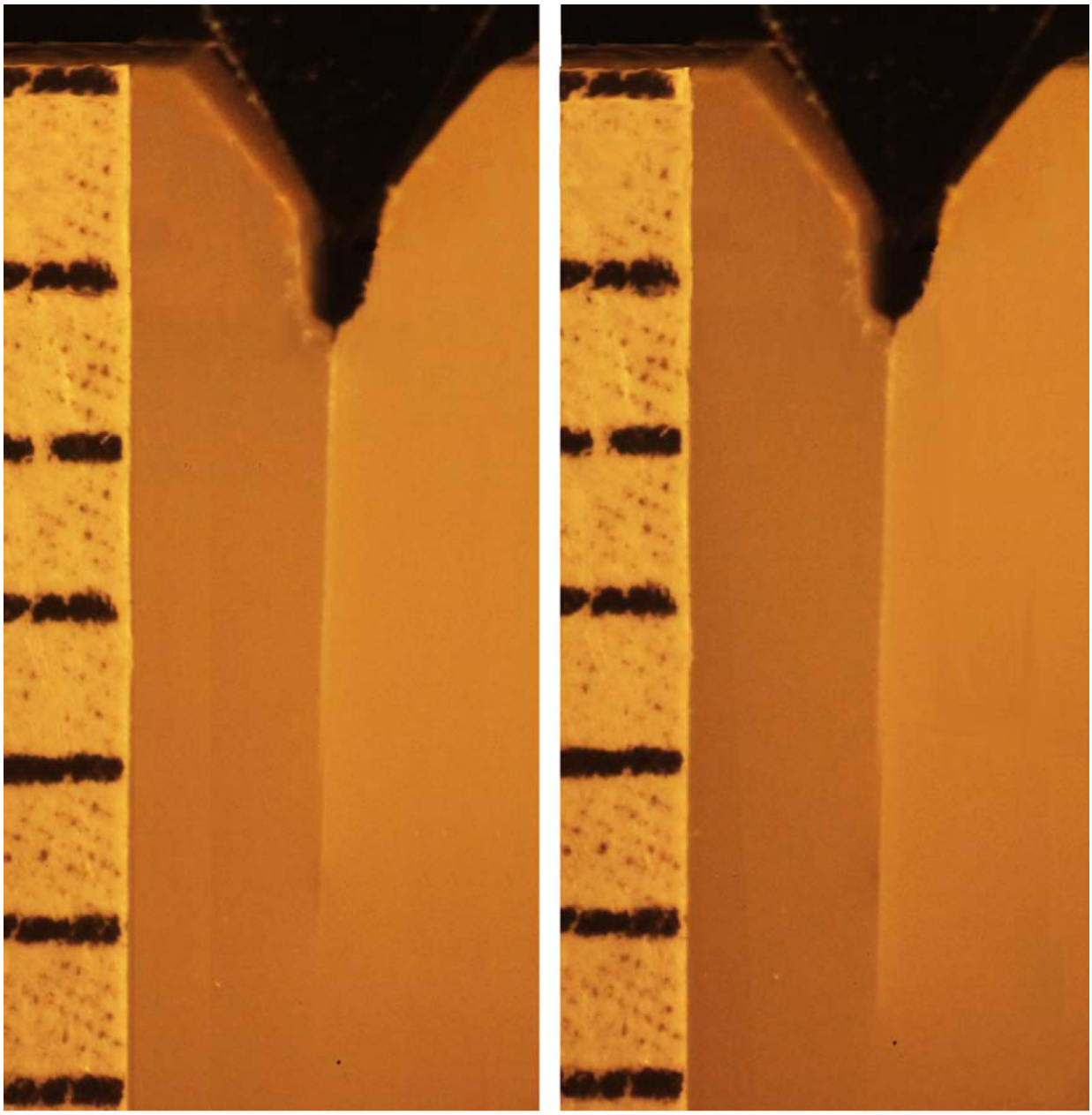

Figure 3.

Two frames from a video sequence corresponding to feldspathic ceramic/resin/feldspathic ceramic specimen. The bright line seen at the specimen center is the crack. The image in (a) and (b) were taken right after a noticeable crack growth occurred and just before the onset of rapid crack growth, respectively.

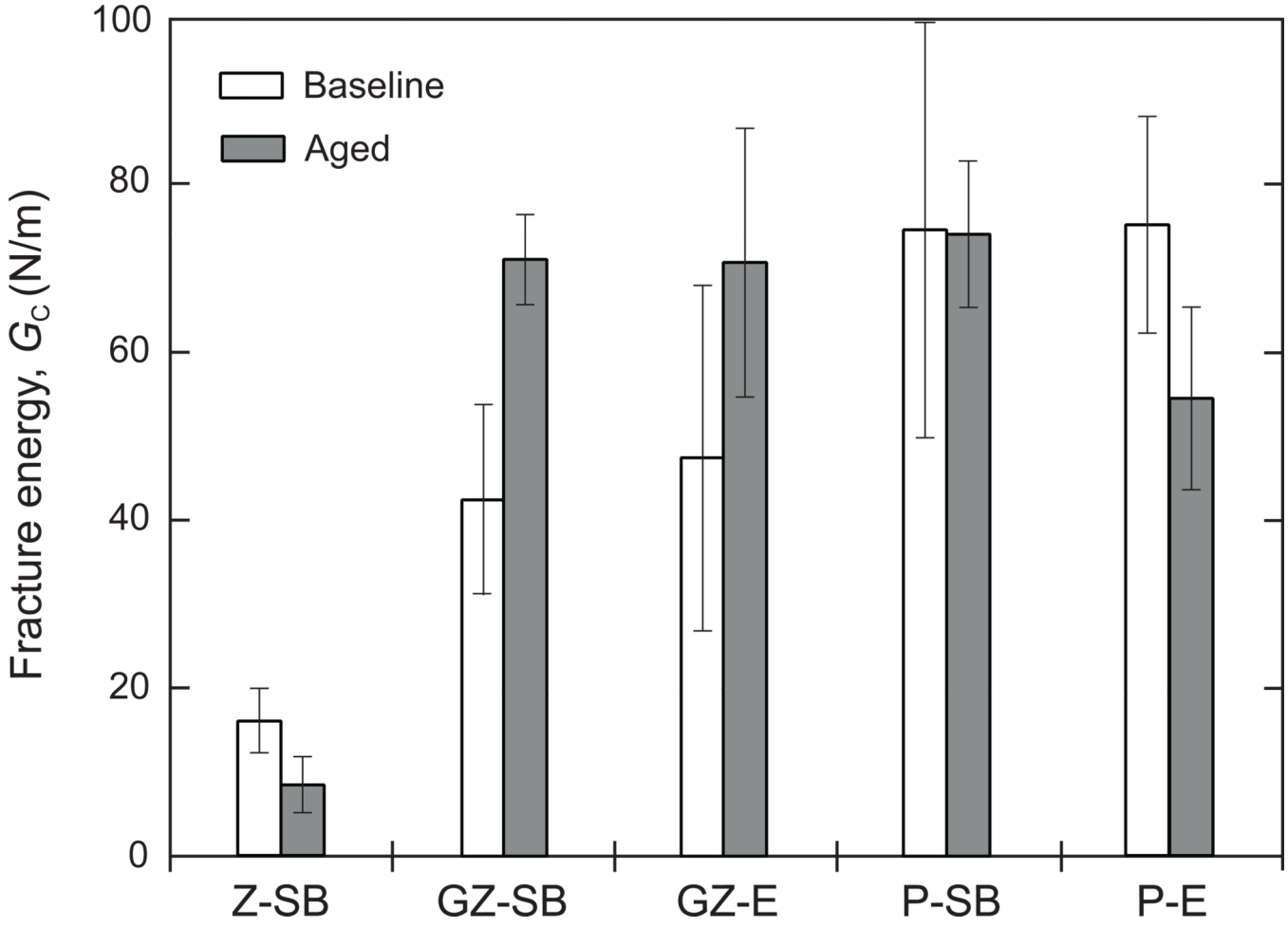

Figure 4.

Bar chart of mean and standard deviation values of fracture energy G_C obtained from all tests performed. The unshaded and shaded bars represent the non-thermocycled/aged and thermocycled/aged specimens, respectively. The abbreviations are defined as follows: Z: zirconia, GZ: graded zirconia, P: feldspathic ceramic, SB: sandblasted, and E: chemically etched. Note that the data for zirconia are well below those for feldspathic ceramic or graded zirconia.

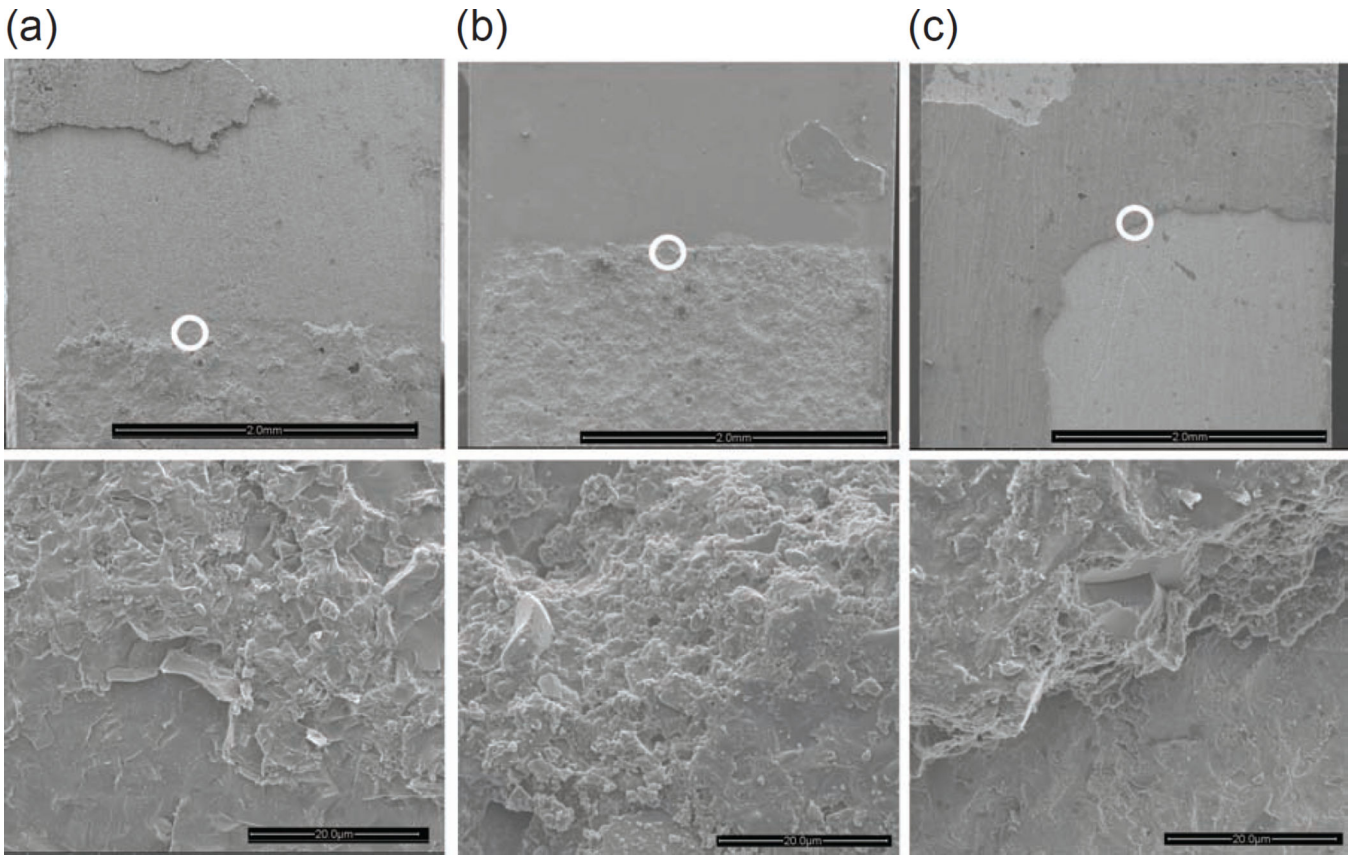

Figure 5.

SEM micrographs of the fractured surfaces of feldspathic ceramic (a), graded zirconia (b) and zirconia (c) bonded dental ceramic specimens, all subjected to sandblasting and thermocycling/aging treatments. The images conclusively correspond to a region slightly ahead of the edge of the crack starter, where slow crack growth followed by a rapid one occurred. The lower images are magnified views of the circled areas in the upper images.

Table 1

Material data in this study.

Material	Young's modulus *E* (GPa)	Poisson's ratio ν
Feldspathic ceramic	63[¥]	0.22[¥]
Zirconia	216[£]	0.30[£]
Graded zirconia	211[£]	0.32[£]
Resin cement	7[¥]	0.35

[¥] Manufacturers' data sheets.

[£] Measured using the ultrasonic method.

Table 2

Mean (standard-deviation) for interfacial fracture energy G_C [N/m].

	Z-SB	GZ-SB	GZ-E	P-SB	P-E
Baseline	16.1 (3.9)^{D}	42.3 (11.4)^{C}	47.6 (20.6)^{BC}	75.1 (24.9)^{A}	75.7 (13.4)^{A}
Aged	8.4 (3.3)^{E}	71.1 (5.5)^{A}	70.8 (16.0)^{AB}	74.5 (8.6)^{A}	54.6 (11.1)^{ABC}

The abbreviations are denoted as follows. Z: zirconia, GZ: graded zirconia, P: feldspathic ceramic, SB: sandblasted, and E: chemically etched. Distinct superscript letters indicate significant difference among groups.